

FINAL REPORT

**STRUCTURAL LOAD TESTING AND FLEXURE ANALYSIS
OF THE ROUTE 701 BRIDGE IN LOUISA COUNTY, VIRGINIA**

Jeremy Lucas

Graduate Research Assistant

**Charles E. Via, Jr. Department of Civil and Environmental Engineering
Virginia Polytechnic Institute & State University**

Thomas E. Cousins, Ph.D., P.E.

Associate Professor

**Charles E. Via, Jr. Department of Civil and Environmental Engineering
Virginia Polytechnic Institute & State University**

Michael C. Brown, Ph.D., P.E.

Research Scientist

Virginia Transportation Research Council

Stephen R. Sharp

Research Scientist

Virginia Transportation Research Council

D. Stephen Lane

Senior Research Scientist

Virginia Transportation Research Council

Virginia Transportation Research Council
(A Cooperative Organization Sponsored Jointly by the
Virginia Department of Transportation and
the University of Virginia)

Charlottesville, Virginia

June 2004
VTRC 04-R12

DISCLAIMER

The contents of this report reflect the views of the authors, who are responsible for the facts and the accuracy of the data presented herein. The contents do not necessarily reflect the official views or policies of the Virginia Department of Transportation, the Commonwealth Transportation Board, or the Federal Highway Administration. This report does not constitute a standard, specification, or regulation.

Copyright 2004 by the Commonwealth of Virginia.

ABSTRACT

A continuous slab bridge in Louisa County, Virginia, on Route 701 developed a planar horizontal crack along the length of all three spans. This project was designed to determine if the current load rating of the bridge could be raised and to document the behavior and stiffness of the bridge to serve as a benchmark for possible future tests, which may determine if there is progressive damage attributable to crack growth.

These objectives were accomplished through field tests performed in November 2003. One truck (loaded to three different weights) was used to perform static and dynamic tests on the bridge, and the truck was oriented in three test lanes. Vertical displacement gages (deflectometers) attached to the underside of the bridge slab were used to measure deflections during the truck passes.

The recorded deflections were analyzed and normalized to document the behavior of the bridge. The values were also compared to estimated design values in accordance with the American Association of State Highway and Transportation Officials' *Standard Specifications for Highway Bridges*.

Under the testing loads, the bridge behaved elastically, and thus raising the load rating of the bridge was considered safe. The deflections and process are presented to allow comparisons with future tests to determine if there is progressive damage to the bridge attributable to crack growth.

FINAL REPORT

STRUCTURAL LOAD TESTING AND FLEXURE ANALYSIS OF THE ROUTE 701 BRIDGE IN LOUISA COUNTY, VIRGINIA

Jeremy Lucas

Graduate Research Assistant

**Charles E. Via, Jr. Department of Civil and Environmental Engineering
Virginia Polytechnic Institute & State University**

Thomas E. Cousins, Ph.D., P.E.

Associate Professor

**Charles E. Via, Jr. Department of Civil and Environmental Engineering
Virginia Polytechnic Institute & State University**

Michael C. Brown, Ph.D., P.E.

Research Scientist

Virginia Transportation Research Council

Stephen R. Sharp

Research Scientist

Virginia Transportation Research Council

D. Stephen Lane

Senior Research Scientist

Virginia Transportation Research Council

INTRODUCTION

Slab bridges have been around for most of the twentieth century. With the advantages of a simplified layout and the requirement for less formwork, compared with other reinforced concrete bridge designs they have been a popular choice where materials were cheap and labor was more expensive. Continuous slab bridges are adaptable to smaller stream crossings and grade separations. They are most economical and popular as three- to five-span configurations with middle span lengths of 35 to 45 ft.

In the early 1980s, the Virginia Department of Transportation (VDOT, 1982) constructed a continuous slab bridge on Route 701 across the Little River, approximately 1.4 miles south of Route 618 in Louisa County, Virginia. The bridge is a three-span continuous reinforced concrete slab bridge with a 15° skew. The end spans are both 40 ft and the center span is 50 ft in length. The spans are haunched toward the piers, with an average thickness of 22.5 in at center span and 33.5 in at the piers. The overall width of the bridge is 29 ft 10 in, with a face-to-face distance between parapets of 28 ft (see Figure 1 and Figure 2).

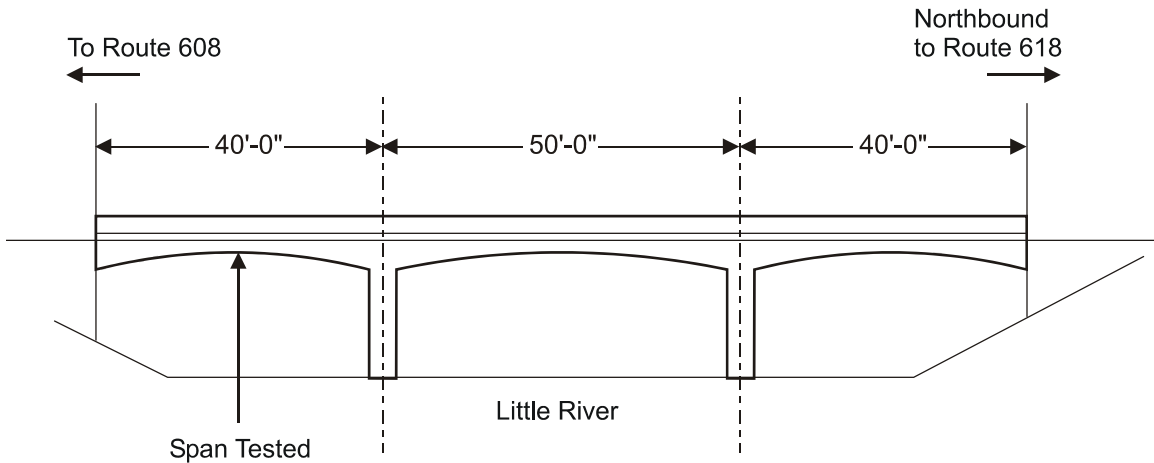


Figure 1. Route 701 Bridge over the Little River.

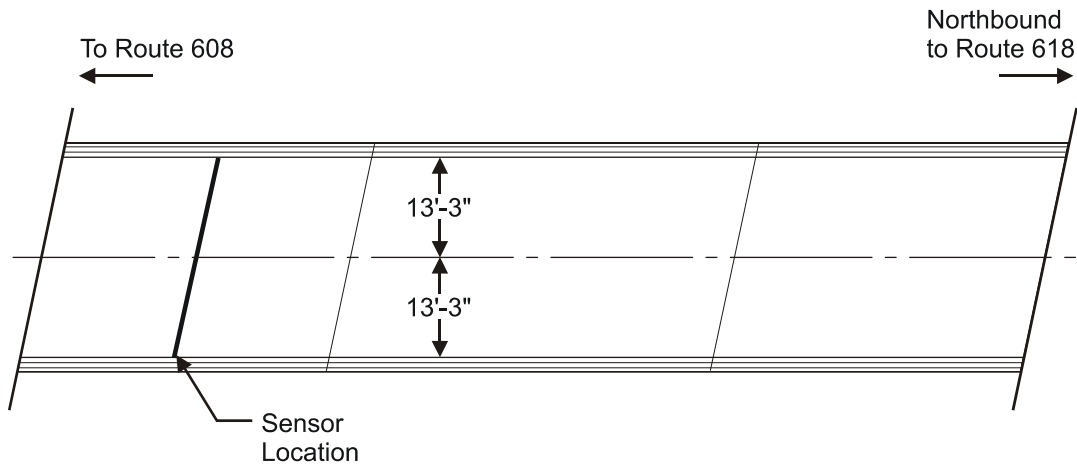


Figure 2. Plan view of Route 701 Bridge.

The bridge was designed in accordance with the American Association of State Highway and Transportation Officials' (AASHTO) *Standard Specifications for Highway Bridges* (1977) and the *Interim Specifications* from 1978 through 1983. The bridge was constructed in accordance with the Virginia Department of Highways and Transportation's *Road and Bridge Specifications* (1982). Grade 60 deformed reinforcing bars were used to reinforce the structure. Class A4 ($f'_c = 4$ ksi) concrete was used in constructing the superstructure.

Following the completion of the bridge in 1985, the Bridge Inspection Report dated October 1987 noted only some vertical cracking with efflorescence in the parapets, some areas of vertical hairline cracking with efflorescence in one of the breast walls, and vertical hairline cracks at the approximate center of both piers.

In February 1996, the report rated the wearing surface and structural condition of the deck in fair condition. The condition description contained the following:

- 4 ea, up to 1/32 in width open longitudinal cracks through deck becoming hairline on bottom.
- Hairline map cracking covering 25% of total deck surface.
- Hairline map cracking with leaching covering 90% of sides of deck.
- Hairline map cracking with leaching covering 40% of total surface of the parapets.
- 1/32 in width open crack leaching efflorescence on sides of deck in built up areas above pier caps at all four locations. A photograph suggests the cracks are roughly horizontal, at approximately mid-depth of the slab.

The January 2000 Structure Inspection Report indicated that the hairline map cracking had spread to 35% of the deck surface and that the mid-depth horizontal cracks had propagated to 15 ft on either side of the piers. The next report, dated January 2002, noted: “up to 1/16” open horizontal crack, entire length of both sides of deck,” and at this point inspection frequency was increased from a 24-month to a 3-month period. In the summer of 2002, during planning for maintenance of the structure, the Virginia Transportation Research Council (VTRC) was asked to determine the cause of the damage and evaluate the condition of the structure.

During the preliminary VTRC survey, concrete cores were obtained for laboratory evaluations. A typical area of map cracking on the deck surface is shown in Figure 3. The horizontal crack, which can be observed on both sides of the deck, is shown in Figure 4 and Figure 5 and varies in width from hairline to 0.25 in. The disposition of this cracking suggested that it had likely propagated through the entire slab. Consequently, the investigators decided to conduct a non-destructive evaluation to determine the extent of the flaw and load testing to assess the structural capacity of the bridge. In the interim, the load rating of the bridge was reduced from 24 tons to 15 tons as a precautionary measure.

PURPOSE AND SCOPE

This project was designed to determine the cause and extent of damage to the deck slab and its structural capacity. Load testing was used to determine if the current load rating of the Route 701 Bridge could be raised. The information found would also serve to document the behavior and stiffness of the bridge and provide a benchmark for future tests, permitting an evaluation of the progression of damage attributable to crack growth.



Figure 3. Route 701 Bridge deck surface.



Figure 4. Crack along length of bridge.

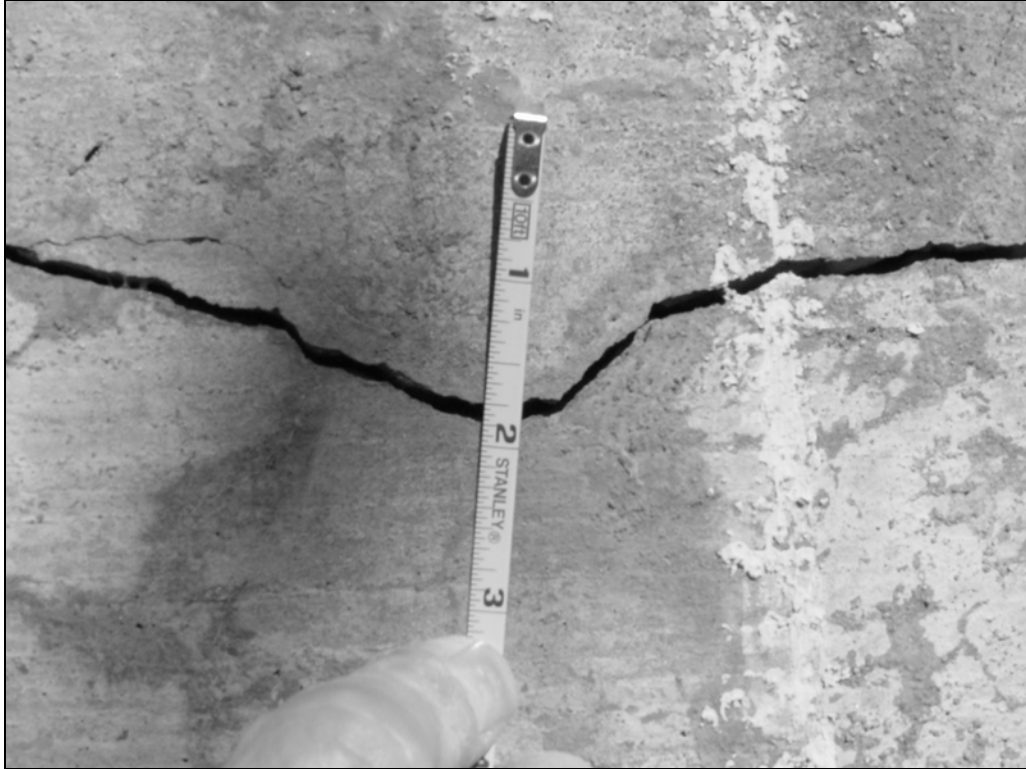


Figure 5. At some locations, crack was 0.25 in at surface.

Specifically, there were three objectives:

1. Determine the cause of the cracking, concrete condition, and extent of the horizontal crack visible on the sides of the slab.
2. Evaluate the existing stiffness and conditions through field testing to determine if the current load rating can be raised.
3. Document the behavior and stiffness of the bridge with the crack through field testing so that future tests can determine if there is progressive damage due to the crack growth.

Concrete cores were obtained to measure the mechanical properties of the concrete and to provide specimens for petrographic examination to determine the cause of the damage. Impact-echo testing was performed to determine if the horizontal crack had propagated through the entire slab. Through field testing, deflections of the bridge under different truck loads were recorded. During various stages of testing, the truck was left empty, partially loaded, or fully loaded; the total load was 26.2, 39.7, and 57 kip, respectively. Normalized deflections under the truckloads were used to determine if there was a linear relationship between load and displacement. Using the truck's weight and dimensions, the applied moment was calculated and compared to the theoretical nominal moment capacity of the bridge. Finally, the deflections were compared to that calculated using the current design specifications. If the bridge behavior

was linear, which indicates that the yield stress of the rebar had not been exceeded under the maximum truckload, then the load rating of the bridge could be raised. In addition, the recorded deflections were used to determine the dynamic load allowance of the bridge.

CURRENT CODE AND SPECIFICATIONS

The current design code for bridges is AASHTO's *Standard Specifications for Highway Bridges* (2002). The slab bridge can be treated as a one-way slab with an effective wheel width. The effective wheel width can be found using Equation 1.

$$E = (4 + 0.06S) \leq 7 \text{ ft} \quad (\text{AASHTO, 2002}) \quad [\text{Eq. 1}]$$

where

E = effective wheel load distribution width on slab (ft)

S = length of span (ft).

According to the code, an effective moment of inertia (Equation 2) can be used to determine deflections.

$$I_e = \left(\frac{M_{cr}}{M_a} \right)^3 I_g + \left[1 - \left(\frac{M_{cr}}{M_a} \right)^3 \right] I_{cr} \leq I_g \quad (\text{AASHTO 2002}) \quad [\text{Eq. 2}]$$

$$M_{cr} = \frac{f_r I_g}{y_t} \quad (\text{AASHTO 2002}) \quad [\text{Eq. 3}]$$

where

I_e = effective moment of inertia (in^4)

M_{cr} = cracking moment

M_a = maximum applied moment

I_g = gross moment of inertia (in^4)

I_{cr} = cracked moment of inertia (in^4)

f_r = modulus of rupture of concrete (psi)

y_t = distance from centroidal axis of the gross section, neglecting reinforcement, to the extreme fiber in tension (in).

Deflection of the concrete can then be found using elastic beam theory.

TEST PROCEDURES

Concrete Cores

Specimens for petrographic examination (ASTM C856), splitting tensile strength (ASTM C496), and electrical resistance (ASTM C1202) were prepared from cores and subjected to testing.

Impact Echo Testing

A DOCTer Impact-Echo Test System was used to determine the flaw depth. This device contained a Mark IV transducer and three impactors (with diameters of 5, 8, and 12.5 mm), which were all positioned on the Star Support frame. Before the flaw depth was estimated, the device was calibrated by determining the propagation velocity of the stress wave in this structure. Because of the uneven bridge deck surface (Figure 3), all impact-echo measurements were made on the underside of the bridge.

Deflection Sensors

Deflection sensors developed and fabricated by Virginia Polytechnic Institute & State University (Virginia Tech) in 1997 were used to measure deflections of the bridge (Figure 6). The sensors were calibrated to the nearest 0.003 in in conjunction with the Optim Electronics MEGADAC data acquisition system and Test Control Software (TCS).

Seven deflection sensors, corresponding to test lanes, were placed on the bridge at midspan of the span on the Route 608 end of the bridge (Figure 1). The deflectometers were bolted to anchors in the concrete through the sensor's base plate. The deflectometers were pre-deflected approximately 0.75 in to allow for relaxation in the deflectometers as the slab displaced downward. The sensors were connected through seven separate channels to the data acquisition system, which was configured for a sample rate of 400 samples per second per channel measuring the change in deflection as the tests are run. A sample of refined data is provided in Figure 7.

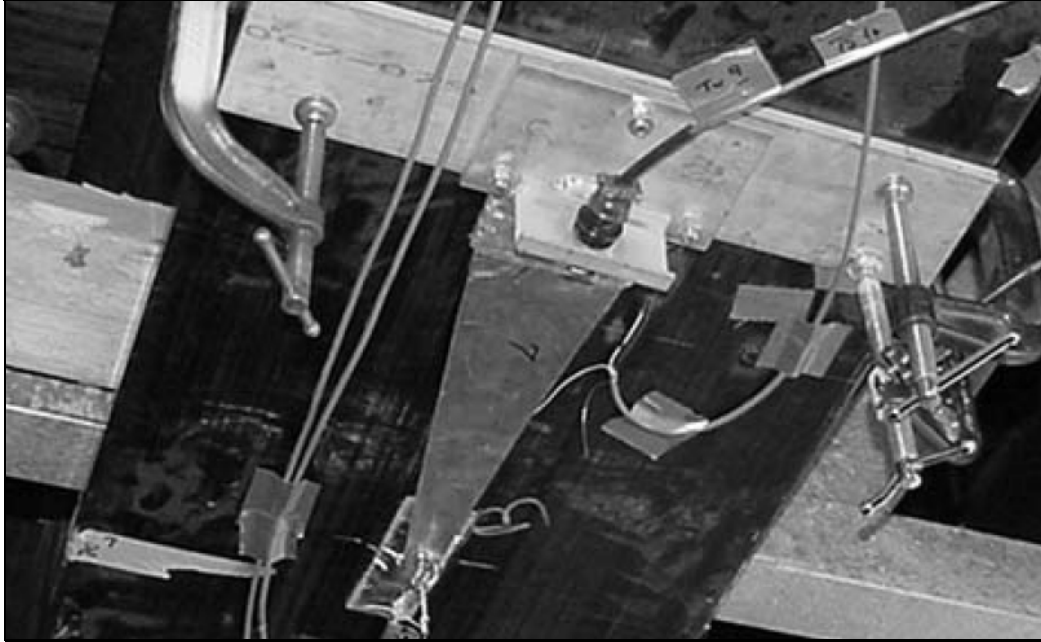


Figure 6. Deflectometer (not on Route 701 bridge).

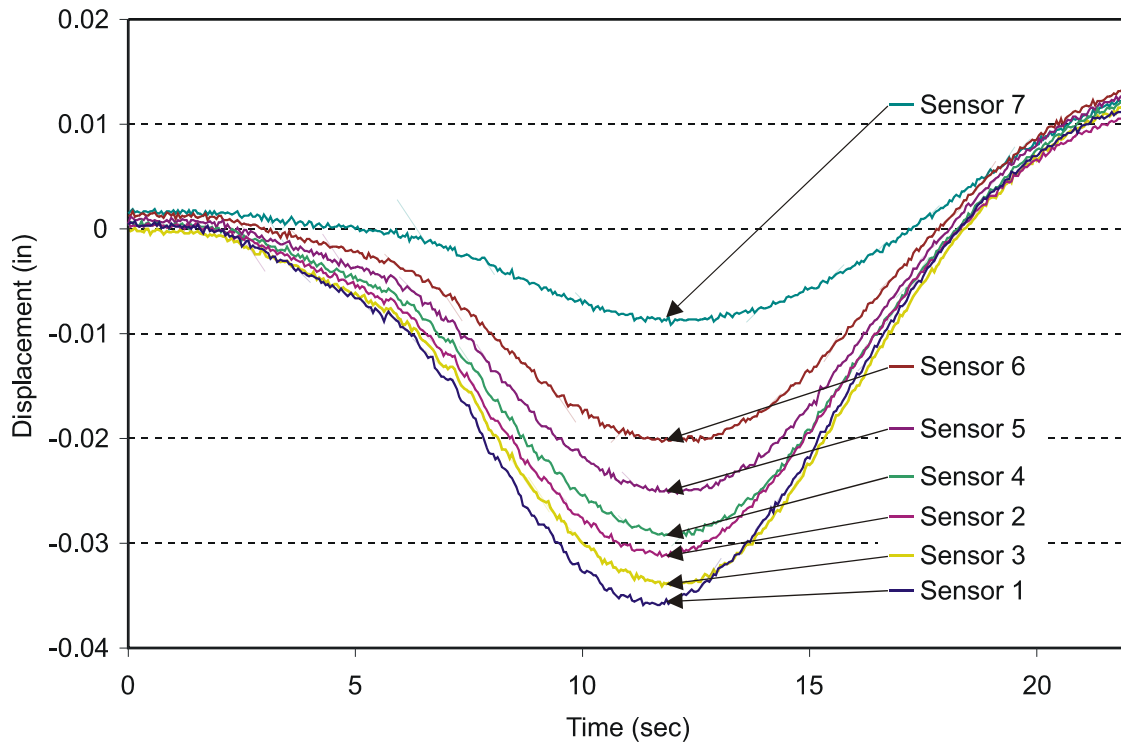


Figure 7. Refined data sample (data set ABRG701A002).

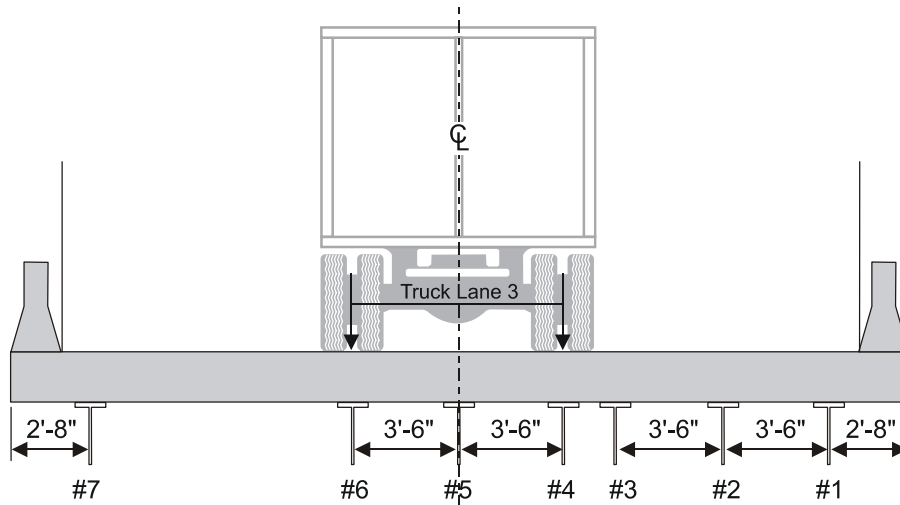


Figure 10. Truck Test Lane 3 (facing northbound).

Truck Description

Figure 11 and Figure 12 show the weight distribution and dimensions of the test truck.

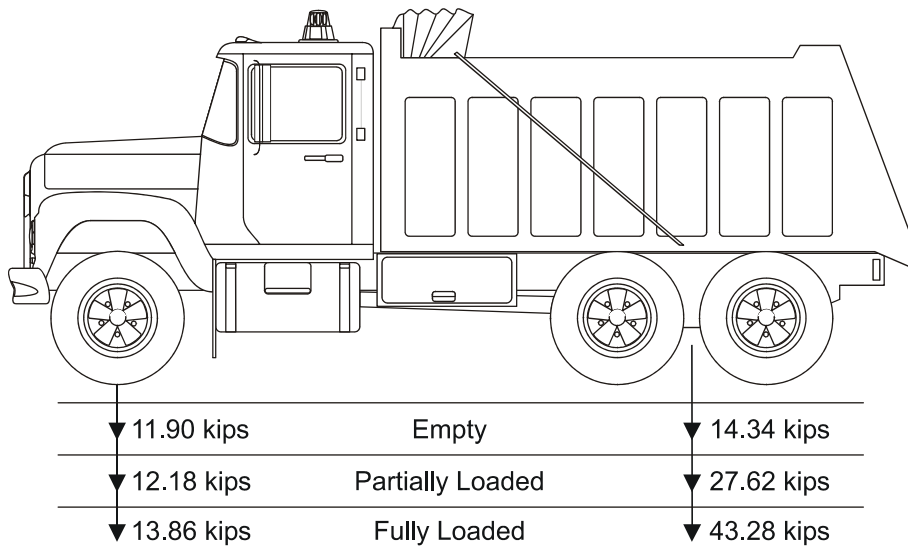


Figure 11. Truck weight distribution when empty (26.2 kips), partially loaded (39.7 kips), and full (57.0 kips).

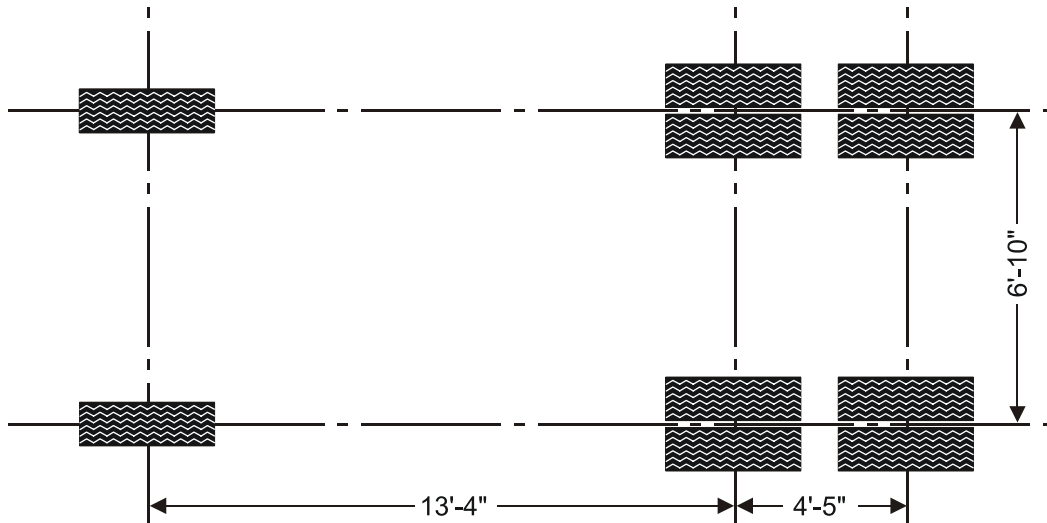


Figure 12. Test truck dimensions.

Test Process

Tests were first run with the truck fully loaded and weighing approximately 57 kips to guarantee a fully pre-cracked section (Figure 13). One mid-span flexural crack was observed on the tested span. There were five “static” tests run on each lane, where the truck, starting and stopping off the span being tested, traveled as slowly as possible along the span of the bridge. There were also six dynamic tests, three in each direction, along Test Lane 3. The truck



Figure 13. Typical truck pass.

speed for these tests was 50 mph. The same tests were then repeated with the truck weight of about 26.2 kips, and then 39.7 kips. The test log is provided in Appendix A.

ANALYSIS AND RESULTS

Concrete Condition

The deck has a grooved surface, and pronounced map cracking had developed. The deck is approximately 22 in deep, and a horizontal crack at mid-depth was visible on both sides of the deck. Two areas of the deck surface retained a thin epoxy leveling overlay.

An examination of cores indicated that the cracks expressed at the surface trended perpendicular to the surface to a depth of about 2 in where they intersected with a network of sub-horizontal cracks (Figure 14). Cracked coarse aggregate particles are associated with the crack network, as are secondary deposits in voids. The aggregate types, quartz sand and gravel, have been associated with damage related to alkali-silica reactivity (ASR) in other structures in the region (Lane, 1993).



Figure 14. Core showing crack from surface extending to depth of approximately 2 in where it connects with sub-horizontal network of cracks associated with coarse aggregate particles.

The secondary deposits in voids were examined in immersion mounts (Figure 15). Examination of thin sections also revealed the secondary deposits lining cracks and voids in the concrete (Figure 16 and Figure 17). The optical properties of the material forming these deposits are consistent with ASR product. The anisotropic character of the reaction products exhibited in these examinations indicates that it has begun to crystallize. ASR products first form as gels that can swell. This swelling can induce significant expansion of the concrete. As the gel begins to crystallize, the swelling tendency is reduced. The damage observed in this deck resulted from expansion caused by ASR of the quartzose gravel aggregate.

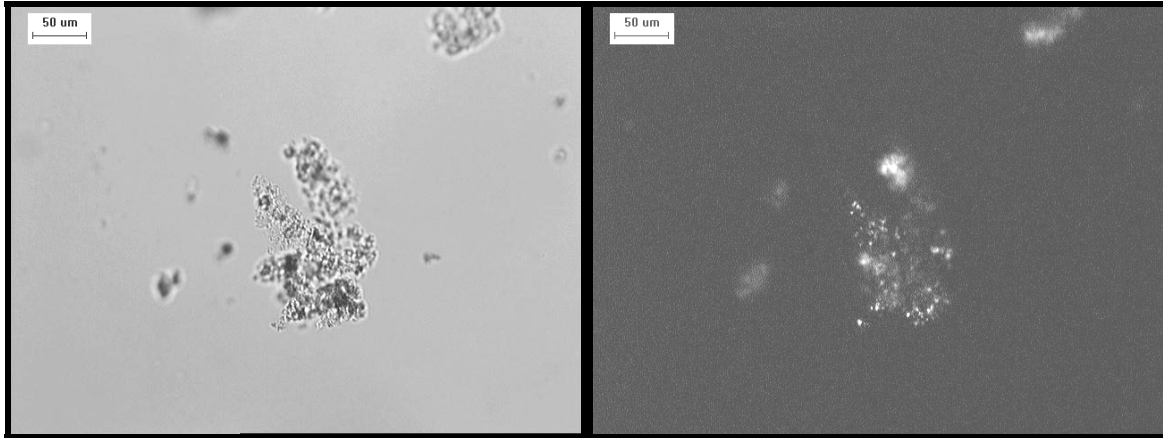


Figure 15. Alkali-silica reaction product from void in concrete. Left image: plane polarized light. Right image: in crossed polarized light material exhibits anisotropic character indicating material has crystallized.

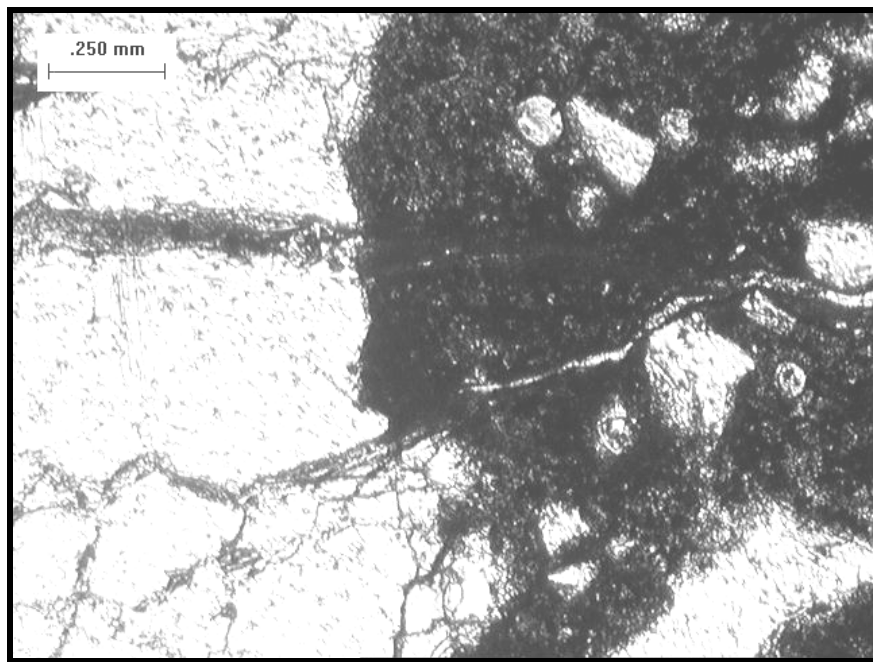


Figure 16. Thin section of concrete showing partially filled crack extending from coarse aggregate particle on left through paste.

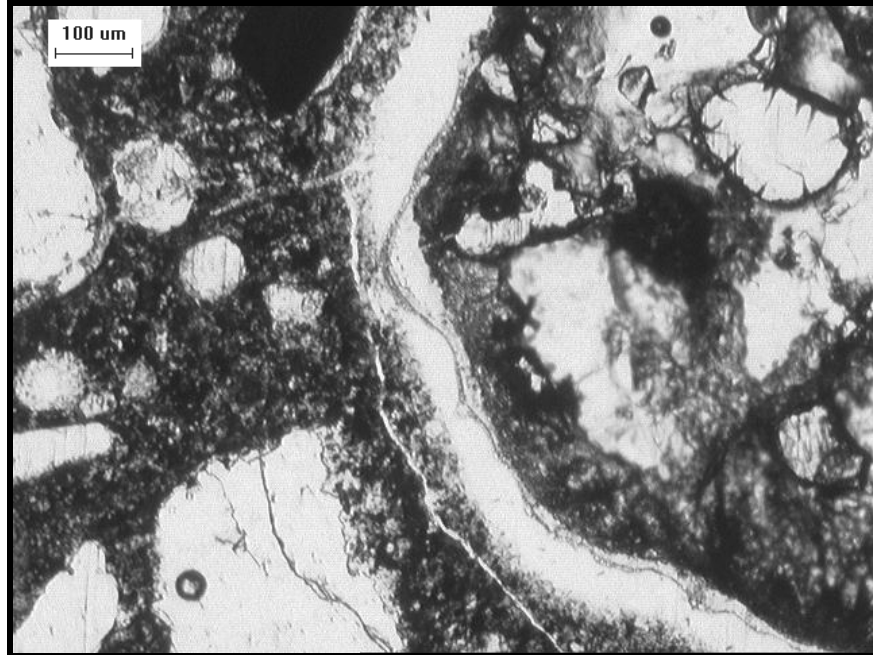


Figure 17. Thin section of concrete showing cracks and voids lined with alkali-silica reaction product.

The splitting tensile test results provide a measure of the extent of internal damage. The average splitting tensile strength of the three cores was 300 psi (Table 1). Assuming that prior to the onset of damage concrete compressive strengths were on the order of 4,000 to 5,000 psi, then splitting tensile strength would be expected to fall in the range of 500 to 600 psi. This suggests a loss in strength of 40% to 50% as a result of internal damage. However, it is important to consider that these results were obtained on cores removed from the structure. The concrete in the structure is under compressive restraint due to expansion, whereas the cores, once removed from the structure, will tend to relax. The core strengths in this relaxed state are thus likely to underestimate significantly the in-situ strength of the deck concrete in a state of compression.

The electrical resistance results provide an indirect indication of the permeability of the concrete. The values fell in the moderate range and were typical of portland cement concretes (Table 1).

Table 1. Results of splitting tensile and electrical resistance tests

Core No.	Splitting tensile (psi)	Electrical Resistance (Coulombs)
3 (span 1, outside wheelpath)	260	---
8 (span 2, wheelpath)	270	---
6 (span 3, inside wheelpath)	380	---
2 (span 1, outside wheelpath)	---	3181
4 (span 2, wheelpath)	---	2192

Bridge Cracks

Although, in general, the underside of the bridge was well suited for making measurements, some regions were inaccessible. Therefore, partial area surveys were performed on the end spans and a full area survey was performed on the center span. A snooper-truck was required in order to access the center span because of the river flowing beneath the bridge. The areas surveyed under each span are illustrated in Figure 18. Impact-echo measurements on all three spans indicated a gap throughout those regions surveyed. A summary of the data collected is provided in Table 2. Based on the impact-echo measurements and the continuous cracks visible along the length of the bridge (Figure 4), a planar crack had more than likely propagated through the entire slab of the bridge.

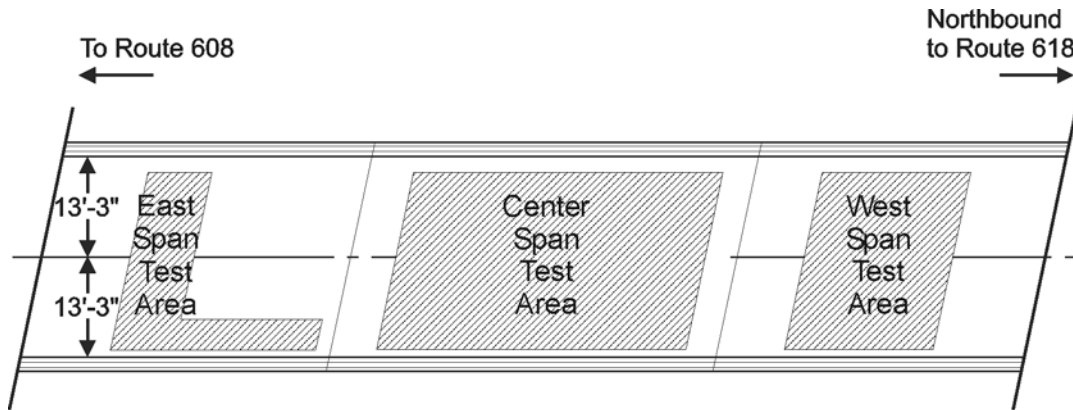


Figure 18. Areas surveyed using impact-echo.

Table 2. Summary of impact-echo measurements (distance from top deck surface, in)

Value	East Span	Middle Span	West Span
Mean	12.5	17.0	12.9
Median	13.8	17.0	13.9
Standard Deviation	3.6	1.6	2.6
Maximum Value	18.8	19.9	17.7
Minimum Value	5.5	12.1	8.2

Maximum Deflections and Normalization

The procedure described herein was performed on all static and dynamic tests. Using Microsoft Excel, the data were visually inspected to determine if all sensors were reporting reasonable trends. A nine-point running average was then used to smooth the data and reduce electronic noise. Figure 19 shows a typical comparison of raw to smoothed data. Maximum deflections were determined for each sensor by finding the maximum point and averaging that with the surrounding points to account for electronic noise (Figure 20). During some runs, the sensors detected the “wobble” of the truck from an uneven approach onto the span; in these cases

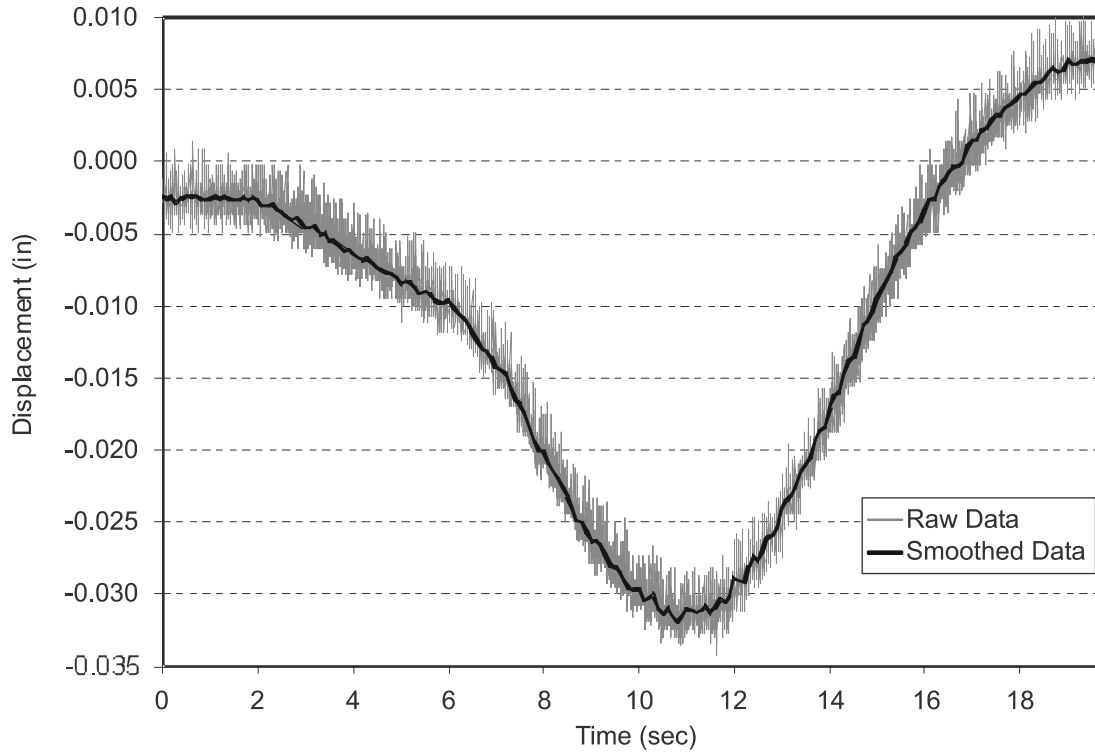


Figure 19. Comparison of raw and smoothed data.

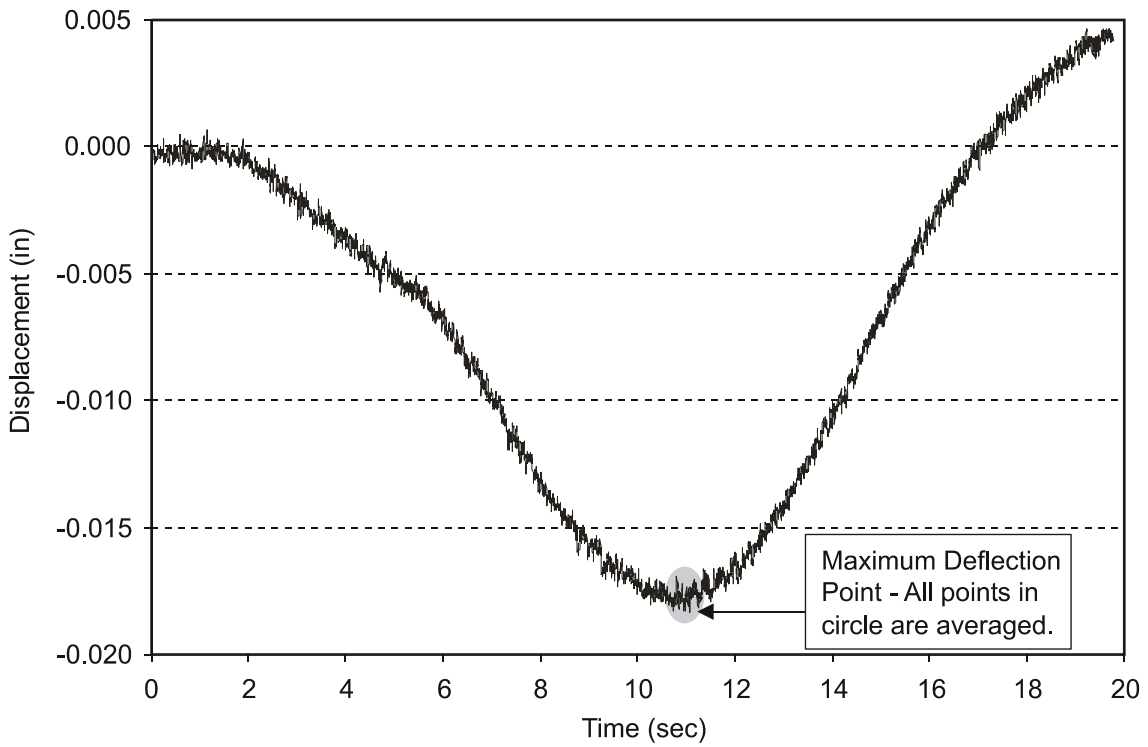


Figure 20. Determining maximum deflection.

the average was found from the local maximum and minimum peak around that point (Figure 21). The maximums were graphed to find the deformed shape of the slab and to ensure that the deflections corresponded to prior assumptions of what the deformed shape should look like (Figure 22).

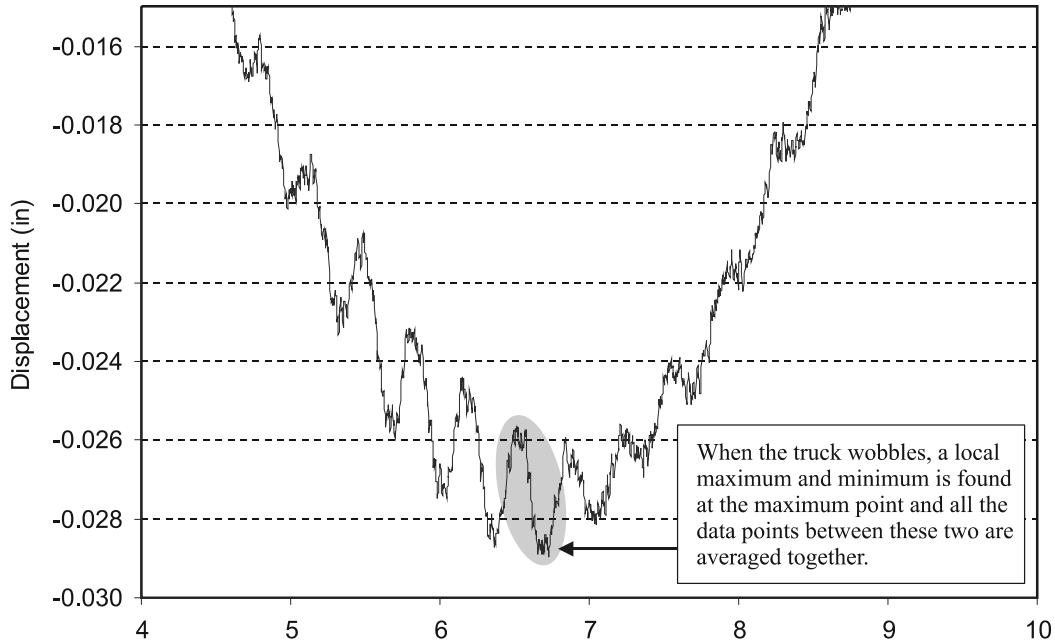


Figure 21. Determining maximum deflection when truck “wobbled.”

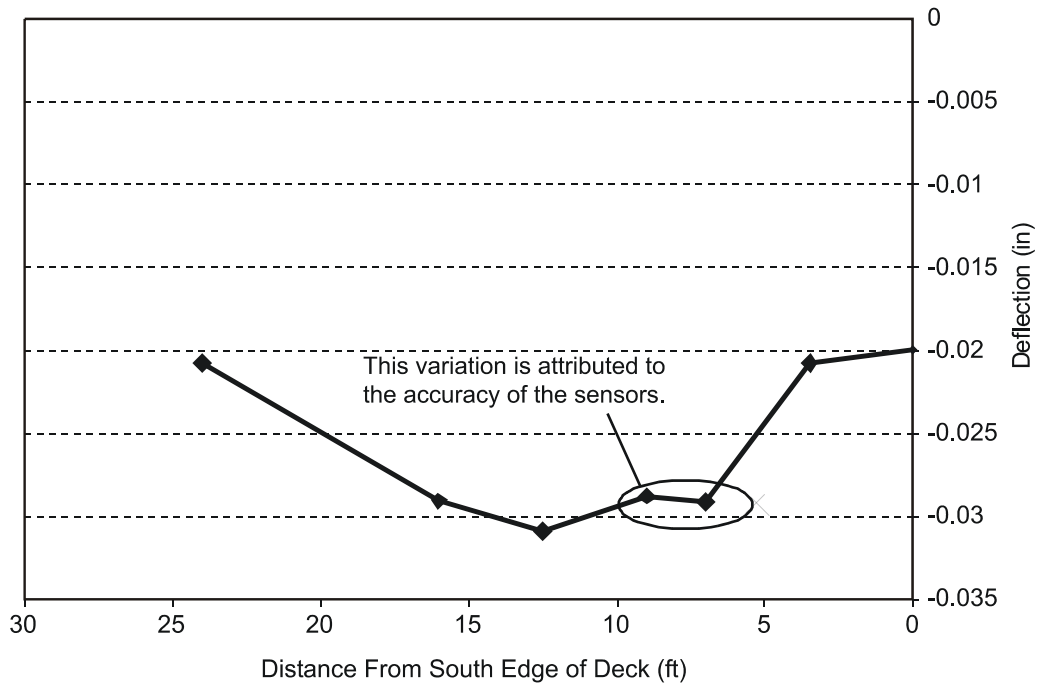


Figure 22. Sample of deformed shape.

The average was taken for all the sensors for each set of tests run. These averages were tabulated and normalized. Normalization was performed by dividing the displacement over the maximum calculated moment at midspan using the dimensions and weight of the truck. The moment was found using continuous beam theory and three points to simulate a wheel line; the space between the three points and weights of each coincide with the test truck dimensions and weights as discussed previously. Deflections and normalized data can be found in Table 3 through Table 9.

Table 3. Average static displacements (in) with truck oriented over Test Lane 1

Truck Load	Sensor Numbers						
	1	2	3	4	5	6	7
Empty	-20.7	-17.7	-20.0	-18.1	-15.6	-12.8	-6.1
Half	-19.1	-16.1	-18.0	-16.4	-13.8	-11.2	-5.6
Full	-20.7	-17.7	-19.9	-17.6	-15.2	-12.2	-6.3

Table 4. Average static displacement (in) with truck oriented over Test Lane 2

Truck Load	Sensor Numbers						
	1	2	3	4	5	6	7
Empty	-5.8	-6.8	-10.6	-11.4	-13.9	-16.1	-20.8
Half	-5.0	-6.0	-9.5	-10.3	-12.3	-14.6	-19.0
Full	-5.6	-6.6	-10.4	-11.0	-13.6	-16.1	-21.1

Table 5. Average static displacement (in) with truck oriented over Test Lane 3

Truck Load	Sensor Numbers						
	1	2	3	4	5	6	7
Empty	-11.9	-12.5	-17.2	-17.3	-18.1	-17.4	-12.7
Half	-10.9	-11.1	-15.7	-15.8	-16.5	-15.8	-10.9
Full	-11.7	-12.2	-17.2	-16.9	-18.2	-17.1	-12.2

Table 6. Average dynamic displacement (in) with truck at 50 mph over Test Lane 3

Truck Load	Direction	Sensor Numbers						
		1	2	3	4	5	6	7
Empty	SB	-0.009	-0.010	-0.013	-0.013	-0.014	-0.013	-0.009
	NB	-0.009	-0.009	-0.013	-0.013	-0.013	-0.013	-0.010
Half	SB	-0.014	-0.015	-0.020	-0.020	-0.021	-0.021	-0.014
	NB	-0.011	-0.012	-0.016	-0.016	-0.017	-0.017	-0.012
Full	SB	-0.027	-0.029	-0.040	-0.040	-0.043	-0.040	-0.028
	NB	-0.021	-0.023	-0.033	-0.033	-0.036	-0.034	-0.025

Table 7. Average normalized displacements (10^{-5} in/kip-ft) with truck over Test Lane 1

Truck Load	Sensor Numbers						
	1	2	3	4	5	6	7
Empty	-0.013	-0.011	-0.013	-0.012	-0.010	-0.008	-0.004
Half	-0.021	-0.018	-0.020	-0.018	-0.015	-0.013	-0.006
Full	-0.035	-0.030	-0.034	-0.030	-0.026	-0.021	-0.011

Table 8. Average normalized displacements (10^{-5} in/kip-ft) with truck over Test Lane 2

Truck Load	Sensor Numbers						
	1	2	3	4	5	6	7
Empty	-0.004	-0.004	-0.007	-0.007	-0.009	-0.010	-0.013
Half	-0.006	-0.007	-0.011	-0.011	-0.014	-0.016	-0.021
Full	-0.010	-0.011	-0.018	-0.019	-0.023	-0.027	-0.036

Table 9. Average normalized displacement (10^{-5} in/kip-ft) with truck over Test Lane 3

Truck Load	Sensor Numbers						
	1	2	3	4	5	6	7
Empty	-0.013	-0.011	-0.013	-0.012	-0.010	-0.008	-0.004
Half	-0.021	-0.018	-0.020	-0.018	-0.015	-0.013	-0.006
Full	-0.035	-0.030	-0.034	-0.030	-0.026	-0.021	-0.011

Dynamic Load Allowance

Dynamic load allowance was calculated using the average maximum dynamic and static displacements for the middle lane under each load case, as seen in Table 10 through Table 12. The maximum and minimum dynamic load allowance factors were also found using the extreme dynamic displacements. Equation 4 was used in determining the factors.

$$DLA = \frac{\Delta_{dyn}}{\Delta_{stat,avg}} - 1 \quad [\text{Eq. 4}]$$

where

DLA = dynamic load allowance factor

Δ_{dyn} = a dynamic displacement

$\Delta_{stat,avg}$ = average static displacement under same load condition.

Table 10. Dynamic load allowance factors for 26.2 kip load

Truck Load	Sensor Numbers						
	1	2	3	4	5	6	7
Minimum	0.107	0.096	0.127	0.122	0.125	0.117	0.064
Average	0.198	0.165	0.177	0.153	0.180	0.169	0.182
Maximum	0.336	0.287	0.245	0.205	0.224	0.227	0.246

Table 11. Dynamic load allowance factors for 39.7 kip load

Truck Load	Sensor Numbers						
	1	2	3	4	5	6	7
Minimum	-0.093	-0.064	-0.081	-0.098	-0.070	-0.098	-0.064
Average	0.033	0.062	0.038	0.038	0.054	0.063	0.070
Maximum	0.244	0.286	0.233	0.243	0.233	0.258	0.208

Table 12. Dynamic load allowance factors for 57 kip load

Truck Load	Sensor Numbers						
	1	2	3	4	5	6	7
Minimum	0.038	0.069	0.085	0.100	0.156	0.176	0.189
Average	0.223	0.247	0.251	0.255	0.281	0.287	0.274
Maximum	0.395	0.413	0.394	0.392	0.416	0.407	0.347

Deflection Calculations According to AASHTO

Some assumptions and simplifications were made to calculate the expected design deflections. The slab was treated as a prismatic member with a constant, average depth of 22.5 in. When determining the cracked moment of inertia, it was assumed that the difference of reinforcing steel between the side and middle lanes was negligible, thus using the same amount of steel for both loading conditions.

Deflections were calculated in accordance with AASHTO (2002) design specifications. The effective moment of inertia was found using Equation 2. The truck's dimensions and weights were used to calculate the moment. The maximum moment was found using continuous beam theory with three moving point loads to simulate the wheel line of a truck. The effective wheel width was found using Equation 1. The hand calculations for determining deflections can be found in Appendix B. The maximum expected deflections for each load case were then calculated using MathCAD[®] spreadsheets developed at Virginia Tech. The maximum deflections were calculated to be 0.33, 0.36, and 0.53 in for the 26.2, 39.7, and 57.0 kip loads, respectively.

Stress in Reinforcement

The stress in the reinforcing steel was calculated using Equation 5. These values were compared to the yield stress of Grade 40 reinforcing steel. Grade 40 reinforcing steel properties were chosen instead of the design Grade 60 properties because of the age of the steel and the weathering the bridge has endured during service. These calculations can be found in Appendix C.

$$\sigma = \frac{My}{I_{cr}} n \quad [\text{Eq. 5}]$$

where

M = applied moment

Y = distance from the neutral axis to location where stress is to be calculated

I_{cr} = cracked moment of inertia

n = modulus ratio between concrete and steel.

The stress in reinforcement was calculated to be 17 ksi under the heaviest loading of 57 kips.

DISCUSSION

Experimental Deflections vs. AASHTO Standard Deflections

The maximum measured deflections were less than 10% of the estimated AASHTO deflections. There are many aspects lending to the difference. For the simplified AASHTO model, many factors affecting the bridge stiffness are ignored. For example, it was considered a prismatic beam, ignoring the haunches at the ends of the spans and the added stiffness from the parapets. Bearings at supports consist of asbestos rubber pads along the bridge seats, rubber or polyvinyl joint filler, and plain steel dowels to resist lateral displacement, and they were assumed not to resist bending forces.

Other factors that could affect the measured deflections are uncertainties in the exact values of the concrete compressive strength and the elastic modulus. These values were taken as design values and likely do not represent the current condition of the concrete. Another factor to consider is that the concrete slab is in a state of compression caused by the restraining effect of the abutments on the slab expansion resulting from ASR.

Normalized Deflections and Bridge Behavior

The normalized data (Table 13) were used to determine if the bridge was acting in a linear, and thus elastic, behavior. Dividing by the maximum applied moment basically gave a slope of the curve of deflections versus applied moments. If this curve is linear, it can be assumed that the bridge is acting in a linear-elastic behavior under the applied loading conditions. Equal normalized deflection values at a certain sensor among all load cases show that this slope is constant. It is probable that the bridge is acting elastically under these load cases; however, the values are very small, making it difficult to state for certain that this is the case.

To confirm further that the bridge is acting elastically, the theoretical design stress of the rebar was measured. Using Grade 40 rebar and a fully cracked section moment of inertia instead of the AASHTO effective moment of inertia leads to a conservative answer, which is 43% of the yield stress, showing the reinforcement is always in the elastic range. This result adds confidence to the elastic behavior found in the normalized deflections.

Table 13. Summary of normalized deflections

Sensor	Truck Oriented Over Lane 1				Truck Oriented Over Lane 2				Truck Oriented Over Lane 3			
	Empty Load	Half Load	Full Load	Var	Empty Load	Half Load	Full Load	Var	Empty Load	Half Load	Full Load	Var
1	-20.7	-19.1	-20.7	1.7	-5.8	-5.0	-5.6	0.8	-11.9	-10.9	-11.7	1.0
2	-17.7	-16.1	-17.7	1.7	-6.8	-6.0	-6.6	0.9	-12.5	-11.1	-12.2	1.4
3	-20.0	-18.0	-19.9	2.0	-10.6	-9.5	-10.4	1.1	-17.2	-15.7	-17.2	1.5
4	-18.1	-16.4	-17.6	1.6	-11.4	-10.3	-11.0	1.1	-17.3	-15.8	-16.9	1.6
5	-15.6	-13.8	-15.2	1.9	-13.9	-12.3	-13.6	1.6	-18.1	-16.5	-18.2	1.7
6	-12.8	-11.2	-12.2	1.6	-16.1	-14.6	-16.1	1.6	-17.4	-15.8	-17.1	1.6
7	-6.1	-5.6	-6.3	0.8	-20.8	-19.0	-21.1	2.1	-12.7	-10.9	-12.2	1.7

Dynamic Load Allowance Factors

There is debate and conflict between AASHTO and other research documents. However, the common maximum impact factor is considered to be approximately 0.3 (Taly, 1998). The average calculated dynamic load allowance of 0.25 with the 57-kip load truck corresponds well with the accepted values. It can be said that the bridge is acting within acceptable and expected dynamic response limits. The maximum measured value was 0.4, which is slightly above expected limits.

CONCLUSIONS

The damage observed in this concrete slab resulted from expansion caused by ASR of the coarse aggregate. The horizontal crack propagated through the slab as internal compressive stresses developed because the abutments restrained longitudinal expansion of the slab. The character of the ASR products suggests that it may be past its major expansive phase.

It is not possible with a single test to determine whether the damage is continuing to progress. To determine this, a future test (or tests) must be performed along with a comparative study against the recorded bridge behavior from this test. The current bridge characteristics of deflection (representing stiffness) and dynamic load allowances under different weights have been documented for comparison with future tests. If future test results do not reveal different characteristics of the bridge, it can be assumed that the bridge performance is not deteriorating over time.

It is important to note that these tests considered only aspects of bridge stiffness and not specific properties or the integrity of any specific material. Through analyses of recorded test deflection data, it was determined that the bridge is behaving elastically under the test loads. The tests performed on the Route 701 Bridge used a maximum truck load of 28.4 tons, which is over the maximum legal limit of 24 tons.

RECOMMENDATIONS

1. *The structure should be reevaluated after 1 to 2 years of additional service to determine whether cracks continue to propagate because of loading or continued material distress related to the observed ASR.* The structure appeared to perform well in its current condition under load testing. However, the significant cracking of the slab compromises its structural integrity and durability. Monitoring the width of the horizontal crack on both sides of the slab will help determine the progress of the damage.
2. *A polymer overlay to seal the surface cracks should be considered.* Such an overlay might help extend the service life.
3. *Because the extensive surface cracking provides pathways for solutions into the slab interior, surface crack repair should be considered.* A gravity-fed resin crack repair using flood-coating is suggested.

ACKNOWLEDGMENTS

The authors acknowledge the support of the Federal Highway Administration for providing the impact-echo test equipment used during this project.

REFERENCES

- American Association of State Highway & Transportation Officials. *Standard Specifications for Highway Bridges*, 17th Ed. Washington, DC, 2002.
- Lane, D.S. *Alkali-silica Reaction in Virginia*. VTRC 94-R17. Virginia Transportation Research Council, Charlottesville, 1993.
- Talley, N. *Design of Modern Highway Bridges*. McGraw-Hill, New York, 1998.
- Virginia Department of Highways & Transportation. Road and Bridge Specifications. Richmond, 1982.
- Virginia Department of Highways & Transportation. *As-Built Plans, Bridge on Rte. 701 Over Little River, Louisa County*. Project 0701-054-119, B606. Culpeper, 1984.

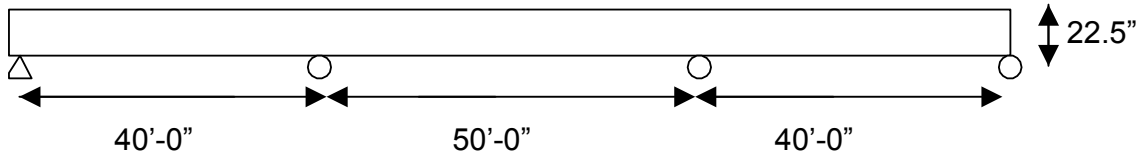
APPENDIX A: TEST LOG

Data Set	Direction	Lane	Speed	Run #	Comments	
002	Northbound	1	Static	1	Full Load Truck	
003	Northbound	1	Static	2		
004	Northbound	1	Static	3		
005	Northbound	1	Static	4		
006	Northbound	1	Static	5		
007	Northbound	1	Static	6		
008	Northbound	3	Static	1		
009	Northbound	3	Static	2		
010	Northbound	3	Static	3		
011	Northbound	3	Static	4		
012	Northbound	3	Static	5		
013	Northbound	2	Static	1		
014	Northbound	2	Static	2		
015	Northbound	2	Static	3		
016	Northbound	2	Static	4		
017	Northbound	2	Static	5		
018	Northbound	2	Static	6		
019	Southbound	3	50 mph	1		
020	Northbound	3	50 mph	2		
021	Southbound	3	50 mph	3		
022	Northbound	3	50 mph	4		
023	Southbound	3	50 mph	5		
024	Northbound	3	50 mph	6		
026	Northbound	1	Static	1		Empty Truck
027	Northbound	1	Static	2		
028	Northbound	1	Static	3		
029	Northbound	1	Static	4		
030	Northbound	1	Static	5		
031	Northbound	3	Static	1		
032	Northbound	3	Static	2		
033	Northbound	3	Static	3		
034	Northbound	3	Static	4		
035	Northbound	3	Static	5		
036	Northbound	2	Static	1		
037	Northbound	2	Static	2		
038	Northbound	2	Static	3		
039	Northbound	2	Static	4		
040	Northbound	2	Static	5		
041	Southbound	3	50 mph	1		
042	Northbound	3	45 mph	2		
043	Southbound	3	50 mph	3		
044	Northbound	3	50 mph	4		
045	Southbound	3	50 mph	5		
046	Northbound	3	50 mph	6		
047	Southbound	3	50 mph	7		

Data Set	Direction	Lane	Speed	Run #	Comments
049	Northbound	1	Static	1	Half Load
050	Northbound	1	Static	2	
051	Northbound	1	Static	3	
052	Northbound	1	Static	4	
053	Northbound	1	Static	5	
054	Northbound	1	Static	1	
055	Northbound	3	Static	2	
056	Northbound	3	Static	3	
057	Northbound	3	Static	4	
058	Northbound	3	Static	5	
059	Northbound	3	Static	1	3-Span Run
060	Northbound	2	Static	2	
061	Northbound	2	Static	3	
062	Northbound	2	Static	4	
063	Northbound	2	Static	5	
064	Southbound	2	50 mph	1	
065	Northbound	2	50 mph	2	
066	Southbound	3	50 mph	3	
067	Northbound	3	50 mph	4	
068	Southbound	3	50 mph	5	
069	Northbound	3	50 mph	6	
070	Northbound	3	Static	1	
071	Northbound	3	Static	2	
072	Northbound	3	Static	3	
073	Northbound	3	Static	4	
074	Northbound	3	Static	5	

APPENDIX B
DEFLECTION CALCULATIONS ACCORDING TO AASHTO

“Simplified” Structure (ignoring haunches and parapets)

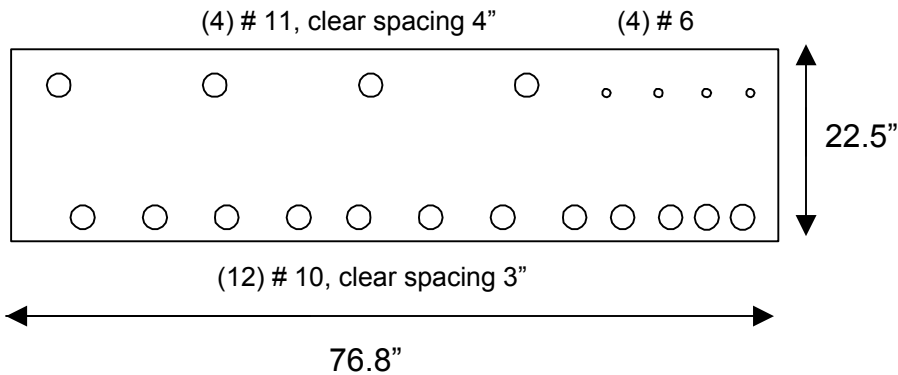


“Effective” Wheel Width

$$E = 4 + 0.06 * S \leq 7.0 \text{ ft}$$

$$E = 4 + 0.06(40 \text{ ft}) = 6.4 \text{ ft, for a } 40' \text{-}0'' \text{ span}$$

Cross Sectional Properties of a 6.4 ft Edge Selection



$f'_c = 4,000$ psi for Class A4

Modulus of Elasticity for concrete: $E_c = 57\sqrt{f'_c} = 57\sqrt{4,000} = 3,600 \text{ ksi}$

Modulus of Elasticity for steel: $E_{st} = 29,000 \text{ ksi}$

$$\text{Modular Ratio: } n = \frac{29,000}{3,600} = 8$$

$$\text{Gross Moment of Inertia: } I_g = \frac{1}{12}(76.8'')(22.5'')^3 = 72,900 \text{ in}^4$$

$$f_r = 7.5\sqrt{f'c} = 7.5\sqrt{4,000\text{ psi}} = 474\text{ psi}$$

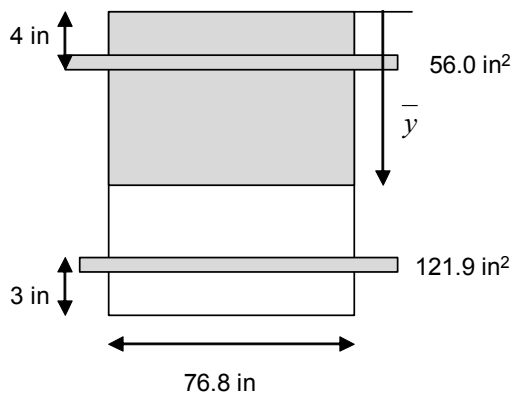
Cracking Moment:
$$M_{cr} = f_r \frac{I}{c_2} = \frac{474\text{ psi} * (72,900\text{ psi})}{11.25"} = 3,000,000\text{ lb-in} = 256\text{ k-ft}$$

Finding Neutral Axis:

Equivalent Area of Compression Steel:

$$A_{st}(n-1) = [(4 * (1.56\text{ in}^2) + 4 * (0.44\text{ in}^2))] * (8-1) = 56.0\text{ in}^2$$

Equivalent Area of Tension Steel: $A_{st}(n) = (12 * (1.27\text{ in}^2)) * 8 = 121.9\text{ in}^2$



$$\sum M_{cg} = 0$$

$$76.8\bar{y}\left(\frac{\bar{y}}{2}\right) + 56.0(\bar{y} - 4) = 121.9(19.5 - \bar{y}) \Rightarrow \bar{y} = 6.23\text{ in}$$

Neglecting Moment of inertia about steel, cracking moment of inertia:

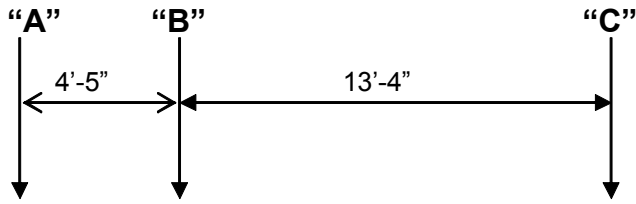
$$I_{cr} = \frac{1}{12}(76.8'')(6.23'')^3 + 6.23''(76.8'')\left(\frac{6.23''}{2}\right)^2 + 56\text{ in}^2(6.23''-4'')^2 + 121.9\text{ in}^2(19.5''-6.23'')^2$$

$$I_{cr} = 28,000\text{ in}^4$$

M_d is the total applied moment at section:

$$DeadLoad = (76.8'' * 22.5'') \frac{1\text{ ft}^2}{144\text{ in}^2} (150 \frac{\text{lb}}{\text{ft}^3}) = 1.8 \frac{\text{k}}{\text{ft}}$$

Using Dr. Beam[®] software, $M_d = 204\text{ k-ft}$ and $M_l = \text{varies upon load}$.



“A” Load	“B” Load	“C” Load	Truck Wt.
10.82 kips	10.82 kips	6.93 kips	57 kips
6.91 kips	6.91 kips	6.19 kips	39.7 kips
3.59 kips	3.59 kips	5.95 kips	26.2 kips

$M_l = 169.7 \text{ k-ft}$ for full load
 $M_l = 111.7 \text{ k-ft}$ for half load
 $M_l = 63.9 \text{ k-ft}$ for empty load

Effective Moment of Inertia:

“Full” Load

$$I_e = \left(\frac{M_{cr}}{M_a} \right)^3 I_g + \left[1 - \left(\frac{M_{cr}}{M_a} \right)^3 \right] I_{cr} = \left(\frac{256}{207 + 169.8} \right)^3 (72,900) + \left[1 - \left(\frac{256}{207 + 169.8} \right)^3 \right] (28,000)$$

$$I_e = 42,081 \text{ in}^4$$

“Half” Load

$$I_e = \left(\frac{256}{207 + 111.7} \right)^3 (72,900) + \left[1 - \left(\frac{256}{207 + 111.7} \right)^3 \right] (28,000) = 51,271 \text{ in}^4$$

“Empty” Load

$$I_e = \left(\frac{256}{207 + 63.88} \right)^3 (72,900) + \left[1 - \left(\frac{256}{207 + 63.88} \right)^3 \right] (28,000) = 65,900 \text{ in}^4$$

Finally, the deflections were found using a deflection program in Mathcad[®].

The predicted deflections for full, half and empty trucks are 0.53”, 0.36” and 0.33” respectively.

APPENDIX C: MAXIMUM STRESS IN REINFORCEMENT

Using $M = 207+170 = 377kip-ft$ as the applied moment.

$I_{cr} = 28,000 in^4$ and $y = 13.3 in$

$$\sigma = \frac{My}{I} * n = \frac{377kip-ft * 13.3in * 12 \frac{in}{ft}}{28,000in^4} * 8 = 17ksi$$

$$\frac{17ksi}{40ksi} = 0.43$$